Physical aging and structural recovery in a colloidal glass subjected to volume-fraction jump conditions

Xiaoguang Peng and Gregory B. McKenna*
Department of Chemical Engineering, Texas Tech University, Lubbock, Texas 79409, USA
(Received 31 August 2015; revised manuscript received 11 December 2015; published 8 April 2016)

Three important kinetic phenomena have been cataloged by Kovacs in the investigation of molecular glasses during structural recovery or physical aging. These are responses to temperature-jump histories referred to as intrinsic isotherms, asymmetry of approach, and memory effect. Here we use a thermosensitive polystyrene-poly (*N*-isopropylacrylamide)-poly (acrylic acid) core-shell particle-based dispersion as a colloidal model and by working at a constant number concentration of particles we use temperature changes to create volume-fraction changes. This imposes conditions similar to those defined by Kovacs on the colloidal system. We use creep experiments to probe the physical aging and structural recovery behavior of colloidal glasses in the Kovacs-type histories and compare the results with those seen in molecular glasses. We find that there are similarities in aging dynamics between molecular glasses and colloidal glasses, but differences also persist. For the intrinsic isotherms, the times t_{eq} needed for relaxing or evolving into the equilibrium (or stationary) state are relatively insensitive to the volume fraction and the values of t_{eq} are longer than the α-relaxation time τ_α at the same volume fraction. On the other hand, both of these times grow at least exponentially with decreasing temperature in molecular glasses. For the asymmetry of approach, similar nonlinear behavior is observed for both colloidal and molecular glasses. However, the equilibration time t_{eq} is the same for both volume-fraction up-jump and down-jump experiments, different from the finding in molecular glasses that it takes longer for the structure to evolve into equilibrium for the temperature up-jump condition than for the temperature down-jump condition. For the two-step volume-fraction jumps, a memory response is observed that is different from observations of structural recovery in two-step temperature histories in molecular glasses. The concentration dependence of the dynamics of the colloidal dispersions is also examined in the equilibrium state and we find that the dynamic fragility index m is sensitive to the degree of softness of the soft colloidal dispersion, indicating that soft colloids make stronger glasses. Finally, we compare the present results with prior findings for similar thermoresponsive systems obtained with diffusing wave spectroscopy and discuss similarities and differences.

DOI: 10.1103/PhysRevE.93.042603

I. INTRODUCTION

In a complex glass-forming fluid, when the relaxation time approaches a range of 1–1000 s, the corresponding range of temperatures or volume fractions is commonly defined as the glass transition region [1–4]. Colloidal dispersions have been considered as model systems in the study of the phase and dynamic behaviors of molecular systems [3]. In the case of molecular glass formers, aging dynamics have generally been studied through temperature down-jump experiments, typically jumping from an equilibrium[1] state in the vicinity of the glass transition temperature T_g to a temperature below T_g that results in an out-of-equilibrium state [5–8]. However, there are also important studies in molecular glasses in which more complicated thermal histories are investigated and the most important of these were cataloged and explored by Kovacs [9,10]. In such experiments, the temperature is the experimental control parameter and one can follow the volume [9,10], enthalpy [11–13], or relaxation time [8,14–16] as a means of examining the nonequilibrium to equilibrium evolution of the glassy system as it ages or its structure recovers. In colloids, on the other hand, the key parameter controlling the phase or dynamic behavior is the volume fraction and not the temperature or, e.g., the volume or enthalpy. Furthermore, unlike temperature in molecular systems, it is difficult to change the volume fraction rapidly and the aging behaviors of colloidal dispersions, i.e., gels and glasses, have generally been examined by using a preshear perturbation at a constant volume fraction or mass concentration and macrorheological and microrheological techniques, i.e., conventional rotary rheometry and light scattering [diffusing wave spectroscopy (DWS)], used to probe the aging dynamics of the disturbed structure of the colloidal dispersions [17–22].

Poly (*N*-isopropylacrylamide), as a thermosensitive polymeric latex, has been used to examine the phase behaviors, from liquid to gel, crystal, and glass, of colloidal dispersions [23,24]. However, there is limited work using temperature-induced volume-fraction up jumps to study the aging behaviors of colloidal glasses [25–29]. We have investigated the differences between temperature-induced volume-fraction up-jump and shear-melting perturbation conditions in Kovacs-type intrinsic isotherms (actually intrinsic iso-volume-fraction) aging kinetics behavior for polystyrene-poly (*N*-isopropylacrylamide)-poly (acrylic acid) (PS-PNIPAM-AA) colloidal glasses [27]. We remark that for molecular glasses aging has generally been studied under isothermal

*Corresponding author: greg.mckenna@ttu.edu

[1]We remark that the use of the term equilibrium is more common in molecular glasses where the supercooled liquid is often considered to be a metastable equilibrium. Also, in the case of some polymeric glass formers, the material cannot crystallize and the liquid state to which the nonequilibrium glass evolves is a true equilibrium state without an underlying crystal equilibrium. We further discuss this later in the text.

conditions [2,5,7,10], but for colloidal glasses aging occurs under iso-volume-fraction conditions [17–22]. In the present work we further investigate the classic Kovacs-type aging behaviors including intrinsic isotherms, memory effect, and asymmetry of approach, for a set of colloidal glasses after temperature-induced volume-fraction jump conditions. The following findings are observed based on results that probe the aging using macrorheology (creep) experiments: (i) aging signature in intrinsic isotherm (intrinsic iso-volume-fraction) experiments, in which the equilibration time t_{eq} for the colloidal glass to evolve into the equilibrium state shows a volume-fraction dependence different from that of the α-relaxation time τ_α; (ii) aging signature in asymmetry of approach experiments, in which asymmetry and nonlinearity of structural recovery occur, but the equilibration times t_{eq} for both volume-fraction down-jump and up-jump conditions are the same; and (iii) aging signature in memory effect experiments, in which the colloidal glass exhibits a memory behavior in a two-step volume-fraction jump history. Similarities and differences in the macrorheology and the DWS microrheology responses are described and discussed and placed into the context of the responses of molecular glasses in similar experiments, including the Kovacs type of temperature jump experiments, but also considering the behavior of molecular glasses subjected to concentration jump (pressure or relative humidity jump) conditions [30–32].

In addition to the nonequilibrium response of this thermoresponsive core-shell colloidal system we also examine aspects of the equilibrium response. In particular we examine the observation that "soft is strong" [33,34] in the sense of dynamic fragility and we compare the results from the macroscopic rheology with the DWS microrheological behavior.

II. EXPERIMENT

A. Synthesis and characterization

The core-shell thermosensitive PS-PNIPAM-AA latex was synthesized through a two-step polymerization. The detailed synthesis procedure and characterization have been described previously [26,35–38]. The weight concentrations of the PS-PNIPAM-AA colloidal dispersions (prepared at 32 °C and adjusted to pH 7.0 with sodium hydroxide solution at this temperature) we used in the current experiments were in a range between 14.0 and 17.0 wt. % in nanowater (directly obtained from Barnstead Nanopure Infinity System, by Thermo Scientific). A sample having a 16.0 wt. % PS-PNIPAM-AA colloidal concentration, the same as previously examined [26,27], was used to study the aging dynamics of the colloidal glass in volume-fraction jump conditions.

The temperature-dependent hydrodynamic diameter of the PS-PNIPAM-AA latex dispersed in nanowater can be described using a linear fit below 34 °C: $D(T) = 244.85 - 1.4869T$, as shown in Fig. 1. Here $D(T)$ is the hydrodynamic diameter of PS-PNIPAM-AA latex at temperature T in degrees Celsius. The size polydispersity of PS-PNIPAM-AA latex is about 25% as measured using dynamic light scattering, effectively preventing crystallization. We remark that the pH of the colloidal systems (0.5 and 5.0 wt. %) was measured and the pH decreased by 0.12 for 0.5 wt. % and by 0.04 for

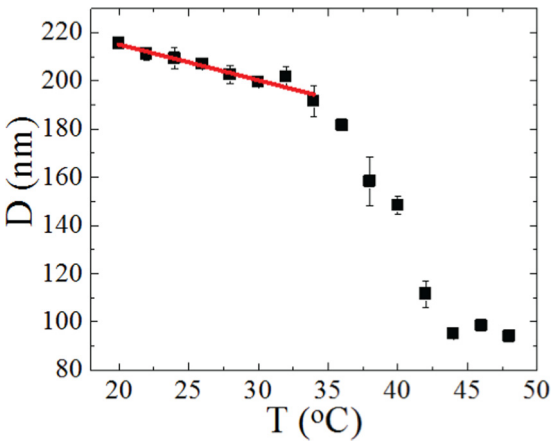

FIG. 1. Temperature dependence of the hydrodynamic diameter of PS-PNIPAM-AA latex in nanowater (data obtained from Di *et al.* [26]). The solid line represents the linear fit $D(T) = 244.85 - 1.4869T$, with T in degrees Celsius.

5.0 wt. % PS-PNIPAM-AA colloidal dispersion. Hence, the pH in the temperature range of interest (33 °C−20 °C) was nearly independent of the temperature. The pH increased 0.6 (±0.1) when the temperature was raised to 50 °C due to the collapse of the shell. However, the hydrodynamic diameter of PS-PNIPAM-AA or PNIPAM-AA latexes at each temperature has been shown to be independent of the pH when the pH is above the pK_a of acrylic acid ($pK_a = 4.25$) [36,39]. For concentrated colloidal samples, i.e., gels and glasses, it is not possible to measure pH due to the solidlike state of the material [39]. Here we only fit the hydrodynamic diameter data in the range that displays a linear temperature dependence. For the purpose of the present study this fit is better than the compressed exponential fit, used previously to describe the full temperature range of the data [26]. The effective volume fraction φ_{eff} (generalized volume fraction [24,33] or packing fraction [40]) of the colloidal system at different temperature was calculated according to the following equation [25,26,41,42]:

$$\varphi_{eff}(T) = \varphi_{eff(collapsed)}[D(T)/D_{collapsed}]^3, \quad (1)$$

where $\varphi_{eff}(T)$ and $\varphi_{eff(collapsed)}$ represent the effective volume fraction φ_{eff} at temperature T and in the collapsed (completely shrunken) state, respectively, $D(T)$ and $D_{collapsed}$ represent the hydrodynamic diameter of the PS-PNIPAM-AA latex particles at temperature T and at the collapsed (completely shrunken) state, respectively, and $\varphi_{eff(collapsed)}$ can be calculated according to the following equation [43]:

$$\varphi_{eff(collapsed)} = \frac{m_{colloid}/\rho_{colloid}}{m_{colloid}/\rho_{colloid} + m_{solvent}/\rho_{solvent}}, \quad (2)$$

where m is the mass of colloids or solvent and ρ is the density of the colloids or solvent. The effective volume fractions $\varphi_{eff(collapsed)}$ for 14.0, 15.0, 16.0, and 17.0 wt. % PS-PNIPAM-AA colloidal dispersion (the particle density is 1.07 g/cm^3) are 0.132, 0.141, 0.151, and 0.161, respectively. The hydrodynamic diameter of PS-PNIPAM-AA latex, measured using light scattering, in the collapsed state $D_{collapsed}$ is 94.1 nm. We remark that the effective volume fraction, not only for

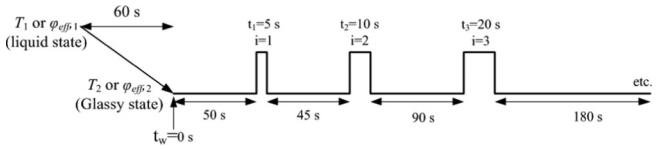

FIG. 2. Struik's protocol for conducting physical aging tests [7,8].

hard-sphere colloidal dispersions but also for soft colloidal dispersions, is difficult to determine due to the flexible particle size and dangling chains [43–46]. A series of methods has been used to measure the effective volume fraction [33,43,47] and there is a large difference between them [47].

B. Rheological measurements

Rheological measurements were conducted using a stress-controlled rotary rheometer (AR-G2, by TA Instruments), in a cone-and-plate geometry. Here the cone diameter was 40 mm and the cone angle was 2° with a fixed truncation gap of 50 μm. The PS-PNIPAM-AA colloidal dispersion in nanowater was surrounded by Krytox 100 oil (by Dupont) to avoid solvent evaporation after the colloidal sample was loaded into the rheometer. For the temperature jump (volume-fraction jump) experiments, the temperature of the environmental chamber was controlled using a liquid nitrogen system. All the experimental temperature (volume-fraction) changes were achieved in less than 60 s.

For the aging experiments, we performed sequential creep experiments following Struik's protocol [7,8] as shown in Fig. 2. We remark that for Struik's protocol the mechanical probe time t_i is less than the aging time or waiting time t_w, usually $t_i \leqslant 0.1t_w$, and also $t_{i+1} = 2t_i$. Here we used $t_i = 0.1t_w$ for all aging tests in this work. After the temperature (volume fraction) of the sample reached the desired temperature (volume fraction), the colloidal glass was left to age for 50 s, followed by a mechanical probe allowed for 5 s (probe time t_i is equal to one tenth of the aging time t_w), and then the colloidal glass was left to age for another 45 s, followed by a second mechanical probe and the probe time (10 s) is one-tenth of previous total aging and probe time (100 s), and so forth.

Importantly, the stress levels for the creep experiments were well within the linear viscoelastic limit. For the dynamic frequency sweeps the stress level was 0.03 Pa and frequency ranged from 3×10^{-4} to 30 rad/s, while for the stress sweep experiments the frequency was 1 rad/s with stress level beginning at approximately 0.01 Pa and the tests run through the onset of nonlinearity or slip; the latter would look like a nonlinearity.

Finally, we comment on the possibility of wall slip in our creep experiments, which is a recognized problem in the measurement of flow in colloidal dispersions [48–50]. Here we remark that there the results are consistent with slip being very small for several reasons. First, we established the range of linear behavior in two ways. The first was the observation from stress sweeps at 1 rad/s, the onset of nonlinear response, often associated with either yield or slip. All of our creep experiments were run at much lower stresses than this threshold, i.e., applied stresses were 0.03–0.4 Pa, while the onset of nonlinearity for the higher concentrations was close to or greater than 1–2 Pa. Furthermore, experiments in which the creep compliance was determined at different stress levels within this linear regime showed that the response was linear, i.e., the creep compliance was independent of applied stress. However, if the slip were linear in applied stress rather than a power law greater than unity as frequently reported [50], this latter response would not be sufficient to ensure that slip was insignificant. Therefore, we also considered the fact that the material in the aging experiments exhibited time-aging time superposition. This being the case and assuming that the slip was independent of aging time, we could estimate that the slip rate was less than approximately 10^{-7} mm/s for an applied stress of 0.1 Pa. Greater slip rates would have lead to a breakdown of the superposability of the creep compliance curves obtained at different aging times. Of interest here is that this rate (and lower) is consistent with extrapolation of the data for slip rates in PNIPAM dispersions tested at stresses above the yield stress [50]. Hence, for the present work slip is not important, but higher stress creep experiments or experiments for longer creep times where one might want to obtain a flow stress or a viscosity could be impacted by slip rates of the order just mentioned.

III. RESULTS

A. Equilibrium behavior

1. Volume-fraction dependence of the dynamics

Importantly, we consider the response of the materials investigated to be in equilibrium when the measured viscoelastic response either does not age or has ceased aging, hence coming to a stationary state. Because of the system polydispersity, crystallization is suppressed, though it may be that at extremely long times a phase separation could occur leading to crystallization. Hence, the observed stationary or equilibrium state is perhaps better considered as a metastable state to which the system evolves. This classification is similar to how the supercooled liquid and glassy states are considered in molecular glasses and especially noncrystallizing polymer glass-forming systems.

The glass transition of the 16.0 wt. % PS-PNIPAM-AA colloidal dispersion was determined by oscillatory tests, as shown in Figs. 3 and 4. Figure 3 show a stress dependence of storage modulus G' and loss modulus G'' as a function of applied stress at a constant frequency of 1 rad/s for several typical different volume fractions. Under low oscillatory stresses, G' and G'' are independent of the applied stress, demonstrating a linear region. When the glass transition is approached, the colloidal system is observed to transition from a liquidlike behavior to a solidlike behavior [40,51,52], viz., G'' dominates at $\varphi_{\text{eff}} = 1.423$, indicating that the colloidal dispersion displays liquidlike behavior. However, at $\varphi_{\text{eff}} = 1.462$, G'' is close to G' and there is a transition between 1.462 and 1.468; solidlike behavior with $G' > G''$ of the colloidal dispersion is observed at $\varphi_{\text{eff}} = 1.468$ or higher.

The results for the frequency dependence of $G'(\omega)$ and $G''(\omega)$ are shown in Fig. 4(a) at three typical different volume fractions, measured in the linear region ($\sigma = 0.03$ Pa). The figure shows that there is a crossover point between $G'(\omega)$

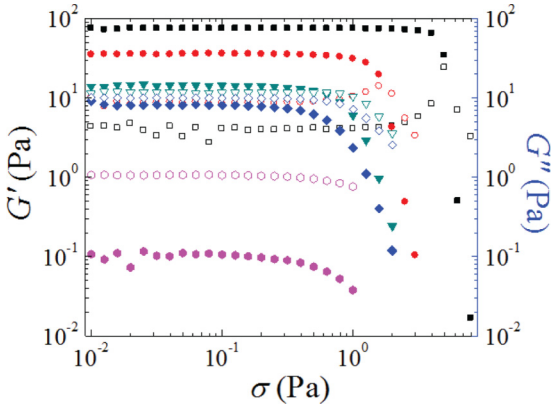

FIG. 3. Stress dependence of storage modulus G' (closed symbols) and loss modulus G'' (open symbols) for the 16.0 wt. % PS-PNIPAM-AA colloidal dispersion at a constant frequency of 1 rad/s at different volume fractions: $\varphi_{\text{eff}} = 1.589$ (26.0 °C) (squares), 1.488 (29.0 °C) (circles), 1.468 (29.6 °C) (down triangles), 1.462 (29.8 °C) (diamonds), and 1.423 (31.0 °C) (hexagons).

and $G''(\omega)$ at each volume fraction and the relaxation time τ_α can be calculated [$\tau_\alpha = 1/\omega$ at $G'(\omega) = G''(\omega)$] [53]. This is the α-relaxation or slow relaxation process [54,55]. With increasing volume fraction, the crossover point shifts to a lower frequency, indicating that the relaxation time τ_α gets longer. Another point of interest is that there is a plateau in $G'(\omega)$ developed as the glass transition is approached [51,52,54–56]. At a volume fraction of 1.436, there is no plateau in $G'(\omega)$. However, there is an obvious plateau developed at a volume fraction of 1.468 and at a higher volume fraction ($\varphi_{\text{eff}} = 1.501$), $G'(\omega)$ becomes nearly independent of the frequency in a wide range. A minimum in $G''(\omega)$ also develops with increasing volume fraction. The inverse of the frequency at the minimum in $G''(\omega)$ corresponds to the β-relaxation or fast relaxation process [54,55], the time for the relaxation of the particle within the cage formed by its neighboring particles, different from that of the α relaxation, in which the particle escapes from its cage.

Figure 4(b) shows a plot of relaxation time τ_α versus the volume fraction and we see that τ_α grows rapidly with increasing volume fraction for the 16.0 wt. % PS-PNIPAM-AA colloidal dispersion. It is well known that the relaxation time and relative viscosity appear to diverge for an ideal hard-sphere colloidal dispersion as the glass transition is approached [3,33]. We can see that there is an approximately 10^4-fold increase in α-relaxation time for a volume-fraction change of 7%. This rapid increase in α-relaxation time is taken as a signature of the approach to the glass transition and similar to a 10^4-fold relative viscosity increase with volume fraction in a hard-sphere colloidal system [3]. The volume fraction of an ideal hard-sphere colloidal dispersion at the glass transition volume fraction φ_g is about 0.58. However, for the soft colloidal dispersions, φ_g is usually above 0.58 and has been reported to be greater than 10 [33] in some systems. The major reason for this difference between the hard-sphere and soft colloidal dispersions in φ_g is the soft and steric interactions and the compressible and interpenetrating shells and layers of the particles [35,40,48]. For the 16.0 wt. % PS-PNIPAM-AA colloidal dispersion, the glass transition volume fraction φ_g is approximately 1.468, corresponding to an α-relaxation time of 6 s. The relaxation time at the glass transition is similar to other soft colloidal dispersions, e.g., for a PS-PNIPAM colloidal system, τ_α is equal to 6 s at the glass transition of 0.77 [51]. For a multiarm polybutadiene star colloidal dispersion, the relaxation time was reported to be approximately 16 s at the glass transition [52]. A much lower relaxation time τ_α of approximately 0.03 s was reported for a PNIPAM-AA dispersion at a volume fraction of 1.405 [47]. Because the glass transition as measured in the laboratory is kinetic, the definition of the τ_α that defines the T_g or φ_g is arbitrary. The requirement is that a consistent definition be used [1–16].

2. *Dynamic fragility*

The concept of dynamic fragility is widely used in molecular glasses to describe the T_g scaled temperature dependence of the relaxation time, in which the fragility is defined at T_g by the logarithmic slope in a renormalized Arrhenius plot [57–60]. Here we apply the same concept in colloidal glasses but use the grass transition volume fraction φ_g instead of T_g. The volume fraction dependences of τ_α for four different weight concentrations are shown in Fig. 5(a) and it can be

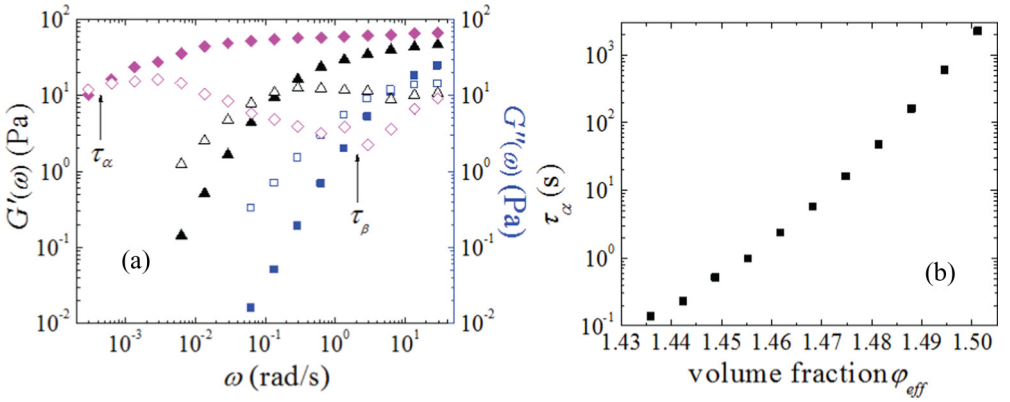

FIG. 4. (a) Frequency dependences of $G'(\omega)$ (closed symbols) and $G''(\omega)$ (open symbols) for the 16.0 wt. % PS-PNIPAM-AA colloidal dispersion at a constant applied stress of 0.03 Pa at three typical volume fractions: $\varphi_{\text{eff}} = 1.436$ (30.6 °C) (squares), 1.468 (29.6 °C) (up triangles), and 1.501 (28.6 °C) (diamonds). (b) Logarithm of relaxation time τ_α versus volume fraction φ_{eff}.

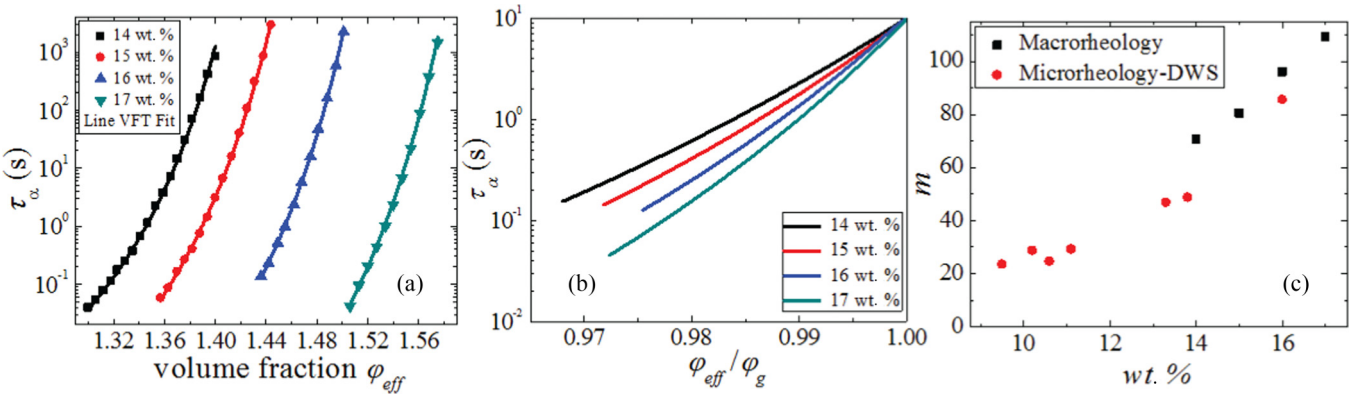

FIG. 5. (a) Logarithm of the relaxation time τ_α versus volume fraction for different weight concentrations of PS-PNIPAM-AA colloidal dispersions. Lines are the modified VFT fits. (b) Relaxation time τ_α versus reduced reciprocal volume fraction for these different weight concentrations of PS-PNIPAM-AA colloidal dispersions near φ_g, with φ_g chosen as the volume fraction at which the relaxation time was 10 s, which is the definition used to calculate the fragility in the glass field [26]. (c) Dynamic fragilities m as a function of the weight concentration for the PS-PNIPAM-AA colloidal dispersions measured by microrheological (DWS) [26] and macrorheological techniques.

seen that the relaxation times increase with increasing volume fraction for all four systems. We remark that the data of Fig. 5(a) do not collapse onto one curve when scaled by φ_g [see Fig. 5(b)]. This is not necessarily surprising as the particles have differing softness (or hardness) because the degree of swelling of the particles varies with temperature, hence there is a different ease of interparticle compression or penetration. It also has been reported by others using a somewhat different approach in which the volume fraction was increased by changing particle number at a constant temperature and this also results in different interparticle compression and penetration [33]. On the other hand, in the case of ideal hard-sphere colloidal dispersions, only one curve of relaxation time or relative viscosity vs volume fraction would be obtained [3]. Figure 5(a) also shows the modified Vogel-Fulcher-Tammann (VFT) [61–63]) fits

$$\ln(\tau) = A + B/(\varphi_\infty - \varphi) \tag{3}$$

for the volume-fraction dependence of the relaxation time at different weight concentrations of the PS-PNIPAM-AA colloidal dispersions and φ_∞ represents the modified VFT divergence volume fraction. The detailed fitting results are given in Table I.

Figure 5(b) shows a plot of the logarithm of the relaxation time τ_α vs the reduced reciprocal volume fraction $\varphi_{\rm eff}/\varphi_g$ for these different weight concentrations of colloidal dispersions. We remark that for determining the dynamic fragility the glass transition volume fraction φ_g is chosen as the volume fraction at which the relaxation time is 10 s, consistent with conventional use in the glass field where T_g is defined, somewhat arbitrarily, as the temperature at which the structural or α-relaxation time takes a value in the range from 1 to 1000 s [1,26,33]. From the modified VFT equation a convenient measurement for the dynamic fragility m in colloidal glasses can be determined through Eq. (2) at φ_g, in analogy to Eq. (3) at T_g, generally used in molecular glasses [57–60],

$$m = \frac{d\log_{10}\tau}{d(\varphi/\varphi_g)} = \frac{B\varphi}{(\varphi_g - \varphi_\infty)^2}, \tag{4}$$

$$m = \frac{d\log_{10}\tau}{d(T_g/T)} = \frac{BT}{(T_g - T_\infty)^2}, \tag{5}$$

where T_∞ is the so-called VFT divergence temperature and B is a material parameter. Here the values of dynamic fragility for the PS-PNIPAM-AA colloidal dispersions range from 80 to 175. This is similar to those generally observed for molecular glasses that range from 20 to 220 [59,60]. These results also agree with the idea that, for colloidal liquids, soft colloids make stronger glass formers [33,34]. At the lower concentrations, the shell of PS-PNIPAM-AA latex has a weaker compression, which leads to a much softer swollen corona than that obtained at the higher concentrations. We remark that for soft colloidal dispersions, each particle is compressed and penetrated by its surrounding neighbors when the effective volume fraction is above 0.64 (random close packing fraction) [33,46]. For the current colloidal dispersions, the higher the concentration, the higher the compression and penetration or the harder the colloid. Figure 5(c) also compares the dynamic fragilities m vs the weight concentration, for the present macrorheological determinations with the results from the DWS microrheological results. We remark that the dynamic fragility data calculated from the plot of the logarithm of τ_α vs the reduced reciprocal volume fraction is lower than those calculated from the plot of the logarithm of τ_α vs reduced reciprocal temperature, which were much higher than the general findings in molecular

TABLE I. The VFT fitting results and dynamic fragility index m for the different weight concentrations of PS-PNIPAM-AA colloidal dispersions.

wt. %	φ_∞	B	φ_g	m
14	1.525 ± 0.012	1.274 ± 0.182	1.368 ± 0.028	79.5 ± 34.0
15	1.576 ± 0.018	1.467 ± 0.357	1.409 ± 0.046	106.6 ± 72.0
16	1.624 ± 0.016	1.514 ± 0.319	1.472 ± 0.040	125.4 ± 80.4
17	1.698 ± 0.020	1.571 ± 0.430	1.549 ± 0.051	174.2 ± 151.1

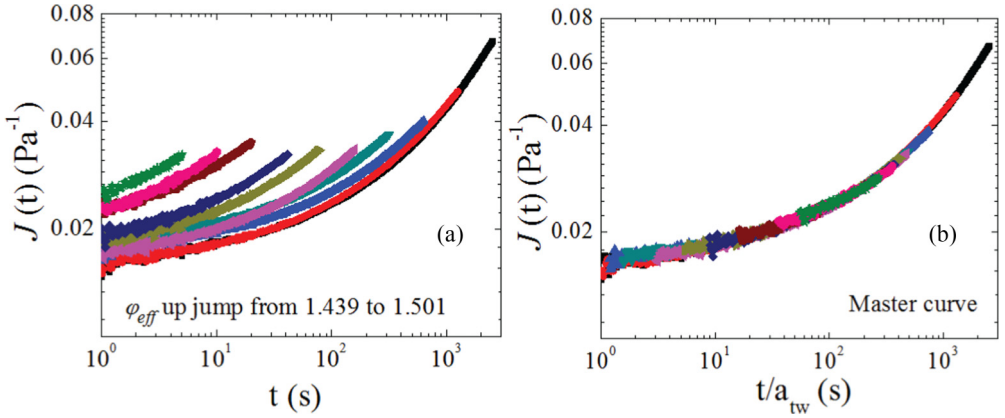

FIG. 6. Aging behavior for the 16.0 wt. % PS-PNIPAM-AA colloidal dispersion after volume-fraction up-jump conditions. (a) Creep compliances during aging after a volume-fraction up jump from 1.439 (30.5 °C) to 1.501 (28.6 °C). From left to right, $t_w = 50$, 100, 200, 400, 800, 1600, 3200, 6400, 12800, and 25600 s (chosen as a reference for constructing a master curve). (b) The master curve was constructed through a horizontal shift. The applied creep probe stress was 0.25 Pa.

glasses [26]. For the colloidal dispersions, it is reasonable to calculate dynamic fragility using volume fraction, rather than the temperature, different from the case in molecular glasses as the controlling parameter is the volume fraction. We see that the dynamic fragility m decreases with decreasing weight concentration (or increasing softness of the colloidal system) for the colloidal dispersions in both instances, though for the same weight concentration the dynamic fragility obtained from macrorheological measurements is somewhat higher than that from the diffusing wave spectroscopy (microrheological) determinations, indicating that slight differences between the two techniques may also persist in the equilibrium state. This issue is discussed further subsequently. A final point to comment upon is that in the present work, while we control volume fraction by changing temperature, the particle size also changes. Hence, the concentration dependences reported here may prove somewhat different from what would be obtained for systems in which the particle size remains constant. A deeper examination of this issue is left to future work.

B. Nonequilibrium behavior

1. Aging signatures: Intrinsic isotherms

In the intrinsic isotherm experiment in molecular glasses [2,5,7,8,10], the temperature is down jumped from above or at to below the T_g and the material aged isothermally. The thermodynamic and the mechanical properties of the materials evolve toward equilibrium with increasing aging time. Kovacs found that the dynamic behavior in the intrinsic isotherm is nonlinear, the structural recovery curves shift rapidly towards longer times with decreasing temperature, and the times needed to reach equilibrium grow rapidly with decreasing temperature [10].

In the present colloid experiments, the volume fraction was jumped from 1.439, in the equilibrium state, to a series of final experimental volume fractions, above φ_g. Figure 6(a) shows the creep responses for the 16.0 wt. % PS-PNIPAM-AA dispersion after volume-fraction up jumps from 1.439 to 1.501. It can be seen that with increasing aging time, the initial creep compliance at 1 s becomes smaller, indicating that aging occurs. These creep compliance curves shift to longer times without changing shape. The equilibrium state (longest aging time) was chosen as a reference and the master curve, as shown in Fig. 6(b), was constructed by simple horizontal shifts, indicating that time-aging time superposition holds for this PS-PNIPAM-AA colloidal dispersion. The shift factors a_{tw} are scaled relaxation times and are defined as [8,31]

$$a_{tw} = \frac{\tau(\varphi_{\rm eff}, t_w)}{\tau(\varphi_{\rm eff}, t_{\rm eq})_r},$$

where $\tau(\varphi_{\rm eff}, t_w)$ and $\tau(\varphi_{\rm eff}, t_{\rm eq})_r$ represent the retardation time for a colloidal glass at aging time t_w and at equilibrium state chosen as a reference, respectively.

The negative logarithm of the aging time shift factor[2] versus the logarithm of aging time at each volume fraction is plotted in Fig. 7(a). We see that the shift factors decrease to a constant value as aging time increases, indicating that the colloidal glass relaxes from the out-of-equilibrium state into the equilibrium state. Here we remark that the time needed to reach equilibrium $t_{\rm eq}$ at a specific aging volume fraction can be difficult to assess and we follow the criteria adopted for volume or enthalpy recovery used by Simon *et al.* [11]. Then the equilibration time $t_{\rm eq}$ is obtained from an arbitrary definition of (near) equilibrium, i.e., the criteria of volume or enthalpy departure from equilibrium at 1×10^{-5}(cm^3/cm^3) or 0.01 J/g, respectively, were used to define the attainment of equilibrium [11]. Here we use the definition that the equilibration time $t_{\rm eq}$ is obtained when the negative logarithm of the aging time shift factor is 0.01, where the equilibrium value is zero.

It is important to remark that the aging kinetics for molecular glasses in the Kovacs-type intrinsic isotherms show equilibration times $t_{\rm eq}$ that get long very rapidly as temperature decreases [14]. Here, on the other hand, the times scale to reach equilibrium for the colloidal glasses is relatively insensitive to the volume fraction, as shown in Fig. 7(b).

[2]We use this convention so that the responses look similar to the volume departure response in the Kovacs type of experiment.

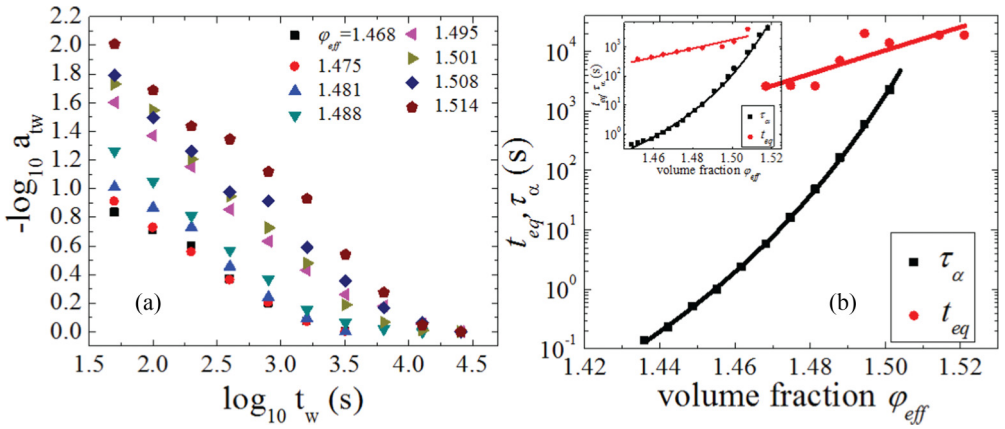

FIG. 7. Aging behaviors for the 16.0 wt. % PS-PNIPAM-AA colloidal dispersion. (a) Plot of the negative logarithm of the aging time shift factors as a function of the logarithm of the aging time for different aging volume fractions. (b) Plot of the logarithm of the relaxation time τ_α and the equilibration time t_{eq} as a function of volume fraction. The inset shows both τ_α and t_{eq} measured with DWS determined from a reanalysis of the data of Di *et al.* [26]. The lines in (b) and the inset are guides for the eye. The applied stresses for the creep probe during aging were 0.03, 0.04, 0.08, 0.12, 0.20, 0.25, 0.35, and 0.40 Pa for the volume fractions in order from 1.468 to 1.514.

The equilibration time t_{eq} increases and does not diverge with increasing volume fraction, while the relaxation times τ_α do. These findings are in agreement with the results obtained from our reanalysis of the microrheology, light-scattering spectroscopy (DWS), experiments reported previously [26] and shown in the inset of Fig. 7(b). We remark that for both soft- and hard-sphere colloidal dispersions, especially at relatively low volume fractions, the differences between the equilibration time t_{eq} and the relaxation time τ_α (the ratio of t_{eq} to τ_α, t_{eq}/τ_α) are usually much larger than those at high volume fraction [25–27,64,65]. Importantly, for hard colloids, these aging behaviors have been generally studied after a shear-melting perturbation, while for the soft colloids studied here, the aging kinetics were determined through temperature-induced volume-fraction up jumps. We remark that there is some work in the literature reporting such a decoupling between relaxation time and equilibration time for colloidal dispersions [25–27,64,65] and the reasons for the decoupling remain unclear. The difference indicates that the structural recovery towards equilibrium seems to represent a longer length or time scale for the process than the process related to the rheological α-relaxation time itself [65]. It is also of interest that the magnitudes of the time differences seen in soft colloids, such as those investigated here, seem to be larger than those seen in hard colloids [25–27,64,65].

The findings in colloidal glasses are different from those in molecular glasses in which both the relaxation time τ_α and the equilibration time t_{eq} change very rapidly, showing a super-Arrhenius behavior with decreasing temperature as T_g is approached [8,66]. We remark that these differences between molecular glasses and colloidal glasses originate from a different history path. For molecular glasses, aging isothermally below T_g, the volume (density) varies with aging time and the volume departure from equilibrium evolves toward zero. In the case of the colloidal glasses, the colloidal system was up jumped from one volume fraction in the equilibrium state to another volume fraction in an out-of-equilibrium state. Although aging occurs, the volume fraction is constant with increasing aging time. We remark that aging for molecular glasses is under isothermal conditions, while for colloidal glasses aging is under iso-volume-fraction conditions.

Figure 7(b) and the inset also show the difference in the equilibration time t_{eq} between macrorheology and microrheology. We see that the equilibration time t_{eq} obtained from both techniques grows with increasing volume fraction. However, the equilibration times t_{eq} from conventional rheometry are longer than those from the DWS microrheology and sometimes up to tenfold longer. Similar results have also been found in molecular glasses [7,11], e.g., for a polyvinyl acetate glass [7], the mechanical measurements take a much longer time to achieve equilibrium, approximately 10^2 times, than do the dielectric measurements at the same investigated temperature. For a polystyrene glass [11], the equilibration time t_{eq} studied from volume recovery measurements are reported to be longer than those from enthalpy recovery measurements. These differences increase with decreasing temperature below T_g but still in what appears to be an equilibrium state because the property of interest had ceased to evolve.

2. *Aging signatures: Memory effect*

For the memory effect in molecular glasses [2,10], the experiment is a two-step temperature history. The material is allowed to partially and isothermally recover before being heated to a higher temperature where the aging occurs. Kovacs found that the volume departure from equilibrium increases from near zero (actual equilibrium state), also called crossover, and passes through a maximum before overlapping with the results for the direct temperature down-jump condition [10]. The physics behind the memory effect are the multiple retardation or nonexponential response of the material and the Boltzmann additivity of the responses in the two-step history. These features can be captured by the Kovacs-Aklonis-Hutchinson-Ramos and Tool-Narayanaswamy-Moynihan models [67–73].

Figure 8(a) shows the results from a two-step volume-fraction history path for the 16.0 wt. % PS-PNIPAM-AA colloidal dispersion. The volume fraction of the PS-PNIPAM-AA colloidal dispersion was first up jumped from 1.439, an

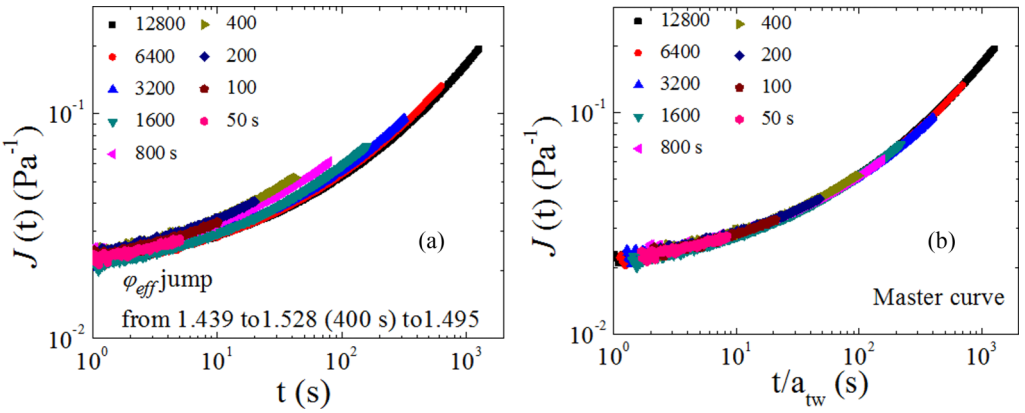

FIG. 8. Creep compliances during aging after a two-step volume-fraction jump for a 16.0 wt. % PS-PNIPAM-AA colloidal dispersion. (a) The volume fraction of the sample jumped from 1.439 (30.5 °C) to 1.528 (27.8 °C) with partial aging for 400 s, followed by a down jump to 1.495 (28.8 °C) and was then left to age. (b) Master curve constructed through a horizontal shift (t_w = 12 800 s was chosen as reference). The creep probe stress during the aging at $\varphi_{\text{eff}} = 1.495$ was 0.20 Pa.

equilibrium state, to 1.528, an out-of-equilibrium state, and the colloidal dispersion was left to partially recover for 400 s. This was followed by a volume-fraction down jump to a final volume fraction of 1.495 where the aging response was monitored by creep experiments using the Struik [8] protocol. The creep curves at each aging time can be superposed onto a single master curve by horizontal shifting, as shown in Fig. 8(b). The creep compliances first shift towards shorter times and then shift towards longer times, i.e., the aging is nonmonotonic, until the equilibrium state is achieved. The nonmonotonicity is shown in the plot of the negative logarithm of the aging time shift factor as a function of the logarithm of the aging time shown in Fig. 9(a). There we see that the negative of the logarithm of the aging time shift factor increases and passes through a peak before overlapping with the results for the single-step volume-fraction up-jump experiment. Two other experiments were also performed: a volume-fraction up jump from 1.439 to 1.562 with partial structural recovery (aging) for 6000 s followed by a volume-fraction down jump to 1.495 and a volume-fraction up jump from 1.439 to 1.596 with partial structural recovery (aging) for 7200 s followed by a volume-fraction down jump to 1.495. These were found to show results similar to those shown in Fig. 9. In the case of structural recovery of molecular glasses [10], the volume departure from equilibrium is observed to start at a near-equilibrium value (near zero) and to increase and pass through a peak before merging with the results for the single-step temperature down-jump condition. The peak position and magnitude depend on the change of temperature. It is unclear at this point whether the peak position dependence is stronger for the molecular glasses (see Ref. [10] for the strength of the peak changes with changing first-step temperature history).

We also carried out experiments at a constant partial aging volume fraction for different partial aging times and these are shown in Fig. 9(b). It can be seen in Fig. 9(b), for this set of experiments (volume-fraction jumps to 1.495 after partial

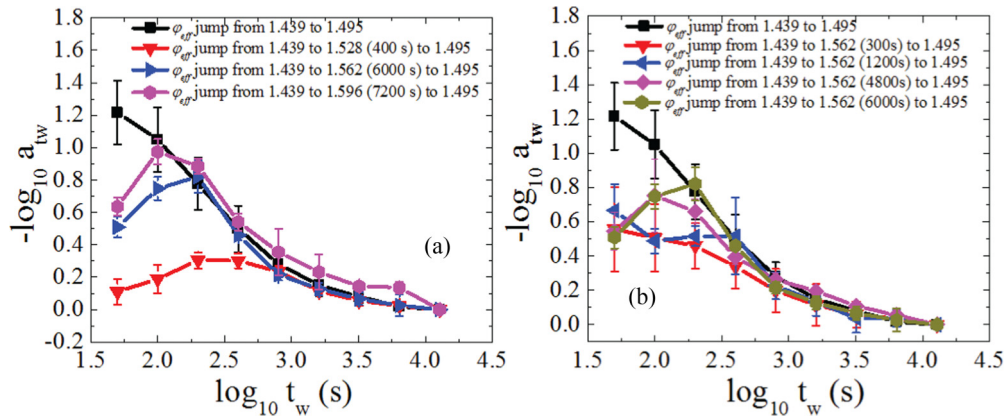

FIG. 9. (a) Plot of the negative logarithm of the aging time shift factor as a function of the logarithm of aging time at 1.495 (28.8 °C) following partial aging histories at three different volume-fraction history paths for the 16.0 wt. % PS-PNIPAM-AA colloidal dispersion: normal volume-fraction up jump to 1.495 (28.8 °C) (squares), partial aging for 400 s at 1.528 (27.8 °C) (down triangles), partial aging for 6000 s at 1.562 (26.8 °C) (sideways triangles), and partial aging for 7200 s at 1.596 (25.8 °C) (hexagons). (b) Partial aging at 1.562 (26.8 °C) followed by a down jump to 1.495 (28.8 °C): normal volume-fraction up jump to 1.495 (28.8 °C) (squares), partial aging time of 300 s (down triangles), partial aging time of 1200 s (sideways triangles), partial aging time of 4800 s (diamonds), and partial aging time of 6000 s (hexagons). Lines are guides for the eye. The creep probe stress for the aging was 0.20 Pa.

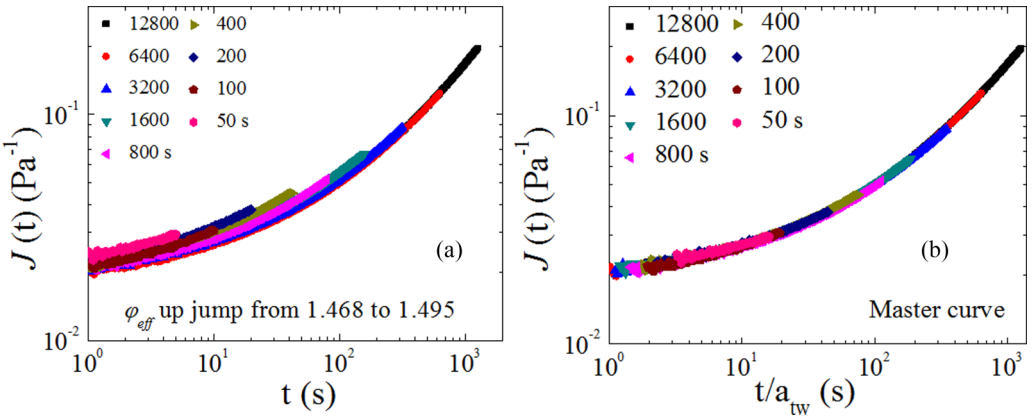

FIG. 10. Creep compliances during aging after a volume-fraction up jump for the 16.0 wt. % PS-PNIPAM-AA colloidal dispersion. (a) The volume fraction of the sample jumped from 1.468 (29.6 °C) to 1.495 (28.8 °C) and was then left to age. (b) Master curve constructed through a horizontal shift (t_w = 12 800 s was chosen as a reference). The creep probe stress was 0.20 Pa.

aging at 1.562), for the short partial aging time (300 s) on the first step, that the negative logarithm of the aging time shift factors decreases monotonically with logarithm of aging time, similar to the results without partial aging. However, with increasing partial aging time, the curves change from this monotonic decrease to a nonmonotonic behavior with the peak position and magnitude only weakly dependent on the partial aging time.

3. *Aging signatures: Asymmetry of approach*

For the asymmetry of approach [2,10], the experiment compares the responses in up-jump and down-jump conditions for temperature steps that are symmetric. However, the volume or enthalpy responses from the two conditions are not mirror images or symmetric. Rather, for the down-jump condition the response is rapid at short times and slows as equilibrium is approached, while for the up-jump condition the response accelerates as volume increases with the approach to equilibrium [2]. This is understood because in the down-jump condition, the material has a higher excess of volume or enthalpy, hence more molecular mobility, at the beginning of the experiment and the molecular mobility decreases as the material densifies and equilibrium is approached. However, for the up-jump condition, the material has a deficit of volume or enthalpy, hence a lower instantaneous mobility that increases as equilibrium is approached. Kovacs also found that the material reaches equilibrium much faster for the down-jump condition than for the up-jump condition [10]. The differences in mobility are understood in terms of a material clock that depends on the free volume or enthalpy state of the material [1,2,4,6,8–10,12–14,16].

In the present experiments, the volume fraction for the 16.0 wt. % PS-PNIPAM-AA colloidal dispersion was jumped from 1.468, at equilibrium, to 1.495, which is initially out of equilibrium, and the aging response followed using the intermittent creep protocol of Struik [8]. This is the up-jump part of the experiment. For the down-jump part of the experiment, the volume fraction for the dispersion was jumped from equilibrium at $\varphi_{\text{eff}} = 1.522$ to $\varphi_{\text{eff}} = 1.495$ and the aging response measured. Figures 10 and 11 show the results for these up-jump and down-jump experiments. In the case of the volume-fraction up-jump experiment, the creep compliance curves shift to longer time, similar to the results for the intrinsic isotherms. For the volume-fraction down-jump experiment, the creep compliance curves shift to shorter times and the initial creep compliance at 1 s increases with increasing aging time. Time-aging time superposition

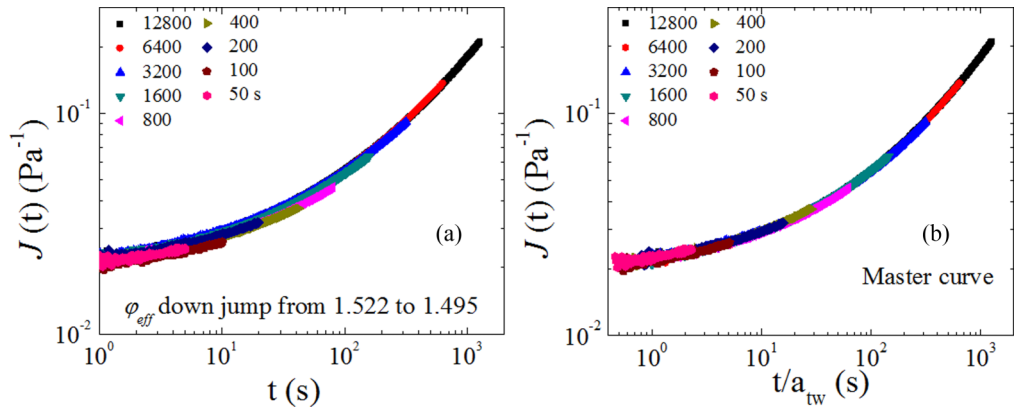

FIG. 11. Creep compliances during aging after a volume-fraction down jump for the 16.0 wt. % PS-PNIPAM-AA colloidal dispersion. (a) The volume fraction of the sample jumped from 1.522 (28.0 °C) to 1.495 (28.8 °C) and was then left to age. (b) Master curve constructed through a horizontal shift (t_w = 12 800 s was chosen as a reference). The creep probe stress was 0.20 Pa.

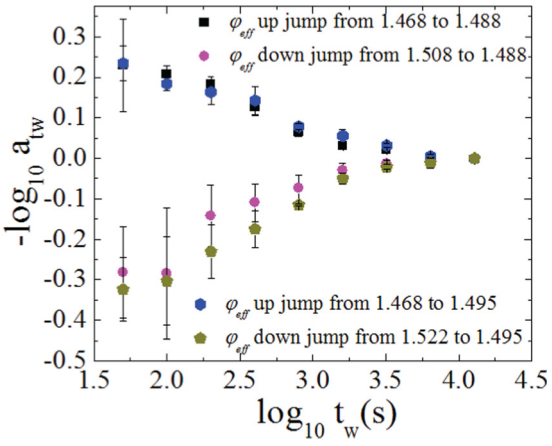

FIG. 12. Plot of the negative logarithm of the aging time shift factor as a function of the logarithm of the aging time for two sets of asymmetry of approach (volume-fraction down jump and up jump of equal magnitude) experiments for the 16.0 wt. % PS-PNIPAM-AA colloidal dispersion: up jump from 1.468 to 1.488 (29.6 °C to 29.0 °C) (squares) and down jump from 1.508 to 1.488 (28.4 °C to 29.0 °C) (circles); up jump from 1.468 to 1.495 (29.6 °C to 28.8 °C) (inverted triangles) and down jump from 1.522 to 1.495 (28.0 °C to 28.8 °C) (diamonds). The creep probe stress was 0.20 Pa.

was found to be valid for both up-jump and down-jump conditions.

Figure 12 shows a plot of the negative logarithm of the aging time shift factor versus the logarithm of aging time for both volume-fraction up-jump and down-jump experiments, in which the negative logarithm of the aging time shift factors show a larger change in the volume-fraction down-jump experiment than in the volume-fraction up-jump experiment. However, the equilibration times t_{eq} for the colloidal system in both volume-fraction up-jump and down-jump experiments are the same, consistent with prior findings using DWS with PNIPAM and PS-PNIPAM-AA colloidal dispersions [25,26], but different from those found for temperature jumps in molecular glasses, in which the equilibration time t_{eq} for the up-jump experiment is longer than that for the down-jump experiment.

IV. DISCUSSION

As a prelude to our discussion of the behaviors of the colloidal system with the molecular system in the Kovacs type of temperature-jump or volume-fraction jump experiments, it is worth commenting that physical aging and the structural recovery also have been investigated in a polymer glass subjected to concentration jump conditions [30–32,74–76]. The concentration jump, i.e., carbon dioxide [32,74,75] or relative humidity (moisture) [30,31], in polymeric glasses can be referred to as a plasticizer jump. In such experiments, the glass transition temperature T_g of the material is varied by changing the plasticizer (small molecules) content, hence there is a concentration glass transition that occurs at constant temperature. Upon revisiting those experiments [30–32] and remarking that there are differences and similarities between temperature jump and concentration jump conditions, we find that it is worth including the results in the present comparisons of molecular glasses in temperature jump conditions with the colloidal system in volume-fraction jump conditions. The differences and similarities among molecular glasses after temperature jump or concentration jump (volume-fraction jump) conditions and those for the colloidal glasses after volume-fraction jumps in the Kovacs-type aging experiments are listed in Table II.

It can be seen that the colloidal glasses and molecular glasses in the different conditions all show signatures in the Kovacs-cataloged histories, but differences persist. (i) For the aging signature in the intrinsic isotherms (intrinsic iso-volume fraction) in the colloidal glasses, the equilibration times t_{eq} are insensitive to the change of volume fraction, but the α-relaxation times exponentially increase with increasing volume fraction. These findings are different from those in molecular glasses after temperature jumps and concentration jumps conditions [2,10,30–32] in which the equilibration time t_{eq} obviously grows rapidly with decreasing temperature or concentration. (ii) The aging signature of asymmetry of approach in the colloidal glass exhibits an equilibration time t_{eq} for both volume-fraction up-jump and down-jump conditions that are nearly the same in the colloidal glasses. This is similar to the findings in concentration jump conditions in molecular glasses [30–32]. However, these findings are different from the temperature jump condition in the molecular glasses where the equilibration time t_{eq} for the up-jump condition is upwards of an order of magnitude longer than that for the down-jump condition [2,10]. (iii) For the aging signature in the memory effect experiments, the colloidal glasses exhibit behavior somewhat similar to that of the concentration jumps in molecular glasses [30–32], but the behavior is different from the response to temperature jumps in molecular glasses. These findings suggest that colloidal glasses in Kovacs-type aging signatures are more similar to molecular glasses after concentration jumps conditions, not the temperature jumps conditions. However, differences still persist.

Additional results of interest stem from the differences and similarities between macrorheological and microrheological behaviors seen in the Kovacs aging signatures for the colloidal glasses. (i) For the aging signature of the intrinsic iso-volume fraction, it is seen that the equilibration time t_{eq} and the structural relaxation times τ_α show a different volume-fraction dependence for both techniques. The equilibration time t_{eq} from the present macrorheological investigation are longer than those seen in the prior DWS or microrheological work [26,27]. This difference in responses is reminiscent of findings in molecular glasses after temperature jump conditions were investigated with different techniques, e.g., mechanical vs dielectric or enthalpic vs volumetric [7,11]. (ii) For the aging signature of asymmetry of approach, the equilibration times t_{eq} for both volume-fraction up-jump and down-jump conditions are the same in colloidal glasses for both techniques. (iii) For the aging signature of memory effect, a clear memory effect was observed in the current colloidal glasses studied using macrorheology to probe the aging response. However, only a weak and first-step independent memory effect was observed for a pure PNIPAM system [25] and no memory effect was seen for the current PS-PNIPAM-AA system [26]. We also find that there are quantitative differences in the dynamic fragility index m and shift factors (scaled relaxation times) obtained

TABLE II. Summary of reported differences and similarities between colloidal glasses and molecular glasses after temperature, concentration, and volume-fraction jumps in the Kovacs aging signature experiments [2,10,25–27,30–32].

System		Kovacs aging signature experiments		
		Intrinsic isotherms	Asymmetry of approach	Memory effect
Molecular glass (temperature jump condition)		t_{eq}[a] increase exponentially with decreasing temperature	t_{eq}[a] for the up-jump condition is longer than that for the down-jump condition	Peak position and magnitude depend on the temperature jump for the temperature jump for the same partial recovery (fictive temperature)
Epoxy glass (concentration jump condition[b])		t_{eq}[a] increase exponentially with decreasing CO_2 pressure or relative humidity	t_{eq}[a] for both CO_2 pressure or relative humidity up-jump and down-jump conditions are similar	Peak position and magnitude are insensitive to the change of the CO_2 pressure or relative humidity
Colloidal glass (DWS)	PNIPAM[c]	t_{eq}[a] (τ_{DWS}) is weakly dependent on the volume fraction of the colloidal system	t_{eq}[a] (τ_{DWS}) for both volume-fraction up- and down-jump conditions are the same	Memory effect is weak and the peak position and magnitude are independent of the change of volume fraction
	PS-PNIPAM AA[d]	For both techniques, τ_α increases exponentially with increasing volume fraction, but t_{eq}[a] (or τ_{DWS}) varies only weakly with volume fraction	t_{eq}[a] (τ_{DWS}) for both up- and down-jump conditions are the same	No memory effect
Colloidal glass (rheometry)			t_{eq}[a] (τ_{DWS}) for both volume-fraction up- and down-jump conditions are the same	Peak position is insensitive to the change of volume fraction, but the magnitude depends on the change of volume fraction

[a]Here t_{eq} is the time, defined more specifically later in the text, to recover into equilibrium rather than the glassy structural relaxation or α-relaxation time.
[b]Concentration jump conditions in a model epoxy glass include two experiments: CO_2 pressure jump [32] and relative humidity jump [30,31] experiments.
[c]Pure PNIPAM particle dispersions. See Ref. [25].
[d]Core-shell polystyrene-PNIPAM-acrylic acid particle dispersions. See Refs. [26,27].

using macrorheology and DWS or microrheology the same volume-fraction colloidal glass [26].

V. CONCLUSION

Equilibrium and nonequilibrium behaviors for a PS-PNIPAAM-AA core-shell colloidal dispersion have been investigated. The volume-fraction dependence of the relaxation time τ_α was studied for a series of different weight concentrations and in the equilibrium state. It was found that the dynamic fragility index m increases as the weight concentration increases, consistent with the idea that soft colloids make stronger glasses. The physical aging and structural recovery behavior were also investigated through a series of volume-fraction up-jump and down-jump experiments and the responses were compared with those of molecular glasses in similar conditions. The aging behaviors in the colloidal glasses investigated here show some of the signatures cataloged by Kovacs for molecular glasses, but differences exist. The specific findings that we report from our macrorheological experiments are observations from the Kovacs type of aging signatures. (i) The times to evolve into equilibrium or the equilibration time t_{eq} in volume-fraction up-jump conditions are relatively insensitive to the increasing volume fraction for the colloidal dispersions, similar to results obtained using a microrheological method (DWS), but differing significantly from the molecular glass where both the relaxation time τ_α and equilibration time t_{eq} obviously increase rapidly with decreasing temperature. The equilibration time t_{eq} is longer than the relaxation time τ_α at the same volume fraction for the macrorheological experiments performed here and the prior works using DWS, a microrheological method. The macrorheological response takes a somewhat longer time to achieve equilibrium than does the DWS measurement at the same volume fraction. (ii) The asymmetry of approach response is observed in both the colloidal dispersion and molecular glasses. However, for both microrheology and macrorheology measurements, the equilibration times t_{eq} for both volume-fraction up-jump and down-jump conditions are the same, similar to results reported for concentration (carbon

dioxide and relative humidity) jumps in a molecular glass, while for the temperature jumps in molecular glasses t_{eq} is considerably longer for the up-jump condition than for the down-jump condition. (iii) The memory effect is also observed in the present colloidal glasses and found to be more similar to the concentration (carbon dioxide and relative humidity) jumps in molecular glasses, but somewhat different from volume-fraction jumps in colloidal glasses studied through microrheology (DWS).

The present results suggest that Kovacs aging kinetics phenomena in molecular glasses after temperature jump or concentration jump conditions and colloidal glasses after volume-fraction jump conditions share similarities, but are different in detail. We further find that the use of diffusing wave spectroscopy, a microrheological method, also gives similarities and differences in behavior compared to the macroscopic rheology. Both sets of findings require further experiment as well as simulation [77] to completely understand the phenomena being observed and establishing the range of validity of the colloidal model for molecular glass-forming systems.

ACKNOWLEDGMENTS

We gratefully acknowledge the National Science Foundation (Grants No. CBET 1133279 and No. CBET 1506072) and the John R. Brandford Endowment at Texas Tech University for partial support of this work.

[1] C. A. Angell, K. L. Ngai, G. B. McKenna, P. F. McMillan, and S. W. Martin, J. Appl. Phys. **88**, 3113 (2000).
[2] G. B. McKenna, in *Comprehensive Polymer Science*, edited by C. Booth and C. Price (Pergamon, Oxford, 1989), Vol. 2, pp. 311–362.
[3] G. L. Hunter and E. R. Weeks, Rep. Prog. Phys. **75**, 066501 (2012).
[4] P. N. Pusey, J. Phys.: Condens. Matter **20**, 494202 (2008).
[5] J. Zhao, S. L. Simon, and G. B. McKenna, Nat. Commun. **4**, 1783 (2013).
[6] P. Badrinarayanan and S. L. Simon, Polymer **48**, 1464 (2007).
[7] J. Zhao and G. B. McKenna, J. Chem. Phys. **136**, 154901 (2012).
[8] L. C. E. Struik, *Physical Aging in Amorphous Polymers and Other Materials* (Elsevier, Amsterdam, 1978).
[9] A. J. Kovacs, J. Polym. Sci. **30**, 131 (1958).
[10] A. J. Kovacs, Fortschr. Hochpolym. Forsch. **3**, 394 (1964).
[11] S. L. Simon, J. W. Sobieski, and D. J. Plazek, Polymer **42**, 2555 (2001).
[12] I. M. Hodge, J. Non-Cryst. Solids **169**, 211 (1984).
[13] C. T. Moynihan, P. B. Macedo, C. J. Montrose, P. K. Gupta, M. A. DeBolt, J. F. Dill, B. E. Dom, P. W. Drake, A. J. Esteal, P. B. Elterman, R. P. Moeller, H. Sasabe, and J. A. Wilder, Ann. NY Acad. Sci. **279**, 15 (1976).
[14] G. B. McKenna and J. Zhao, J. Non-Cryst. Solids **407**, 3 (2015).
[15] I. Echeverria, P. L. Kolek, D. J. Plazek, and S. L. Simon, J. Non-Cryst. Solids **324**, 242 (2003).
[16] J. M. Hutchinson, Prog. Polym. Sci. **20**, 703 (1995).
[17] G. B. McKenna, T. Narita, and F. Lequeux, J. Rheol. **53**, 489 (2009).
[18] J. M. Lynch, G. C. Cianci, and E. R. Weeks, Phys. Rev. E **78**, 031410 (2008).
[19] Y. M. Joshi and G. R. Reddy, Phys. Rev. E **77**, 021501 (2008).
[20] B. Abou, D. Bonn, and J. Meunier, Phys. Rev. E **64**, 021510 (2001).
[21] L. Cipelletti, S. Manley, R. C. Ball, and D. A. Weitz, Phys. Rev. Lett. **84**, 2275 (2000).
[22] E. H. Purnomo, D. van den Ende, S. A. Vanapalli, and F. Mugele, Phys. Rev. Lett. **101**, 238301 (2008).
[23] Z. Meng, J. K. Cho, V. Breedveld, and L. A. Lyon, J. Phys. Chem. B **113**, 4590 (2009).
[24] G. Romeo, A. Fernandez-Nieves, H. M. Wyss, D. Acierno, and D. A. Weitz, Adv. Mater. **22**, 3441 (2010).
[25] X. Di, K. Z. Win, G. B. McKenna, T. Narita, F. Lequeux, S. R. Pullela, and Z. Cheng, Phys. Rev. Lett. **106**, 095701 (2011).
[26] X. Di, X. Peng, and G. B. McKenna, J. Chem. Phys. **140**, 054903 (2014).
[27] X. Peng and G. B. McKenna, Phys. Rev. E **90**, 050301(R) (2014).
[28] E. H. Purnomo, D. van den Ende, J. Mellema, and F. Mugele, Europhys. Lett. **76**, 74 (2006).
[29] P. Yunker, Z. Zhang, K. B. Aptowicz, and A. G. Yodh, Phys. Rev. Lett. **103**, 115701 (2009).
[30] Y. Zheng and G. B. McKenna, Macromolecules **36**, 2387 (2003).
[31] Y. Zheng, R. D. Priestley, and G. B. McKenna, J. Polym. Sci. B **42**, 2107 (2004).
[32] M. Alcoutlabi, L. Banda, S. Kollengodu-Subramanian, J. Zhao, and G. B. McKenna, Macromolecules **44**, 3828 (2011).
[33] J. Mattsson, H. M. Wyss, A. Fernandz-Nieves, K. Miyazaki, Z. Hu, D. R. Reichman, and D. A. Weitz, Nature (London) **462**, 83 (2009).
[34] C. A. Angell and K. Ueno, Nature (London) **462**, 45 (2009).
[35] N. Dingenouts, C. Norhausen, and M. Ballauff, Macromolecules **31**, 8912 (1998).
[36] J.-H. Kim and M. Ballauff, Colloid Polym. Sci. **277**, 1210 (1999).
[37] M. Siebenbueger, M. Fuchs, and M. Ballauff, Soft Matter **8**, 4014 (2012).
[38] Z. Zhou, J. V. Hollingsworth, S. Hong, G. Wei, Y. Shi, X. Lu, H. Cheng, and C. C. Han, Soft Matter **10**, 6286 (2014).
[39] X. Xia and Z. Hu, Langmiur **20**, 2094 (2004).
[40] U. Gasser, J. S. Hyatt, J.-J. Lietor-Santos, E. S. Herman, L. A. Lyon, and A. Fernandez-Nieves, J. Chem. Phys. **141**, 034901 (2014).
[41] H. Senff, W. Richtering, Ch. Norhausen, A. Weiss, and M. Ballauff, Langmuir **15**, 102 (1999).
[42] I. Deike, M. Ballauff, N. Willenbacher, and A. Weiss, J. Rheol. **45**, 709 (2001).
[43] T. Eckert and W. Richtering, J. Chem. Phys. **129**, 124902 (2008).
[44] I. Berndt, J. S. Pedersen, and W. Richtering, Angew. Chem. Int. Ed. **45**, 1737 (2006).
[45] P. N. Segre, S. P. Meeker, P. N. Pusey, and W. C. K. Poon, Phys. Rev. Lett. **75**, 958 (1995).
[46] M. Muluneh, J. Sprakel, H. M. Wyss, J. Mattsson, and D. A. Weitz, J. Phys.: Condens. Matter **23**, 505101 (2011).
[47] S. B. Debord and L. A. Lyon, J. Phys. Chem. B **107**, 2927 (2003).

[48] R. Buscall, J. Rheol. **54**, 1177 (2010).
[49] R. Buscall, J. I. McGowan, and A. J. Morton-Jones, J. Rheol. **37**, 621 (1993).
[50] T. Divoux, V. Lapeyre, V. Ravaine, and S. Manneville, Phys. Rev. E **92**, 060301 (2015).
[51] V. Carrier and G. Petekidis, J. Rheol. **53**, 245 (2009).
[52] B. W. Erwin, S. A. Rogers, M. Cloitre, and D. Vlassopoulos, J. Rheol. **54**, 187 (2010).
[53] J. D. Ferry, *Viscoelastic Properties of Polymers*, 3rd ed. (Wiley, New York, 1980).
[54] J. Mewis and N. J. Wagner, *Colloidal Suspension Rheology* (Cambridge University Press, Cambridge, 2012).
[55] M. E. Helgeson, N. J. Wagner, and D. Vlassopoulos, J. Rheol. **51**, 297 (2007).
[56] T. G. Mason and D. A. Weitz, Phys. Rev. Lett. **75**, 2770 (1995).
[57] C. A. Angell, J. Non-Cryst. Solids **131–133**, 13 (1991).
[58] C. A. Angell, Science **267**, 1924 (1995).
[59] D. Huang and G. B. McKenna, J. Chem. Phys. **114**, 5621 (2001).
[60] Q. Qin and G. B. McKenna, J. Non-Cryst. Solids **352**, 2977 (2006).
[61] H. Vogel, Physik. Zeitschr. **22**, 645 (1921).
[62] G. S. Fulcher, J. Am. Ceram. Soc. **8**, 339 (1925).
[63] G. Tammann and W. Hesse, Z. Anorg. Allg. Chem. **156**, 245 (1926).
[64] D. Masri, G. Brambilla, M. Pierno, G. Petekidis, A. Schofield, L. Berthier, and L. Cipelletti, J. Stat. Mech. (2009) P07015.
[65] D. Masri, M. Pierno, L. Berthier, and L. Cipelletti, J. Phys.: Condens. Matter. **17**, S3543 (2005).
[66] G. B. McKenna, J. Phys.: Condens. Matter **15**, S737 (2003).
[67] A. Q. Tool and C. G. Eichlin, J. Am. Ceram. Soc. **14**, 276 (1931).
[68] A. Q. Tool, J. Am. Ceram. Soc. **29**, 240 (1946).
[69] A. Q. Tool, J. Am. Ceram. Soc. **31**, 177 (1948).
[70] O. S. Narayanaswamy, J. Am. Ceram. Soc. **54**, 491 (1971).
[71] C. T. Moynihan, A. J. Easteal, D. C. Tran, J. A. Wilder, and E. P. Donovan, J. Am. Ceram. Soc. **59**, 137 (1976).
[72] M. A. Debolt, A. J. Easteal, P. B. Macedo, and C. T. Moynihan, J. Am. Ceram. Soc. **59**, 16 (1976).
[73] A. J. Kovacs, J. J. Aklonis, J. M. Hutchinson, and A. R. Ramos, J. Polym. Sci. B **17**, 1097 (1979).
[74] G. K. Fleming and W. J. Koros, Macromolecules **19**, 2285 (1986).
[75] M. Alcoutlabi, L. Banda, and G. B. McKenna, Polymer **45**, 5629 (2004).
[76] G. B. McKenna, J. Non-Cryst. Solids **353**, 3820 (2007).
[77] R. N. Zia, B. J. Landrum, and W. B. Russel, J. Rheol. **58**, 1121 (2014).